COMBUSTION ENGINEERING, INC.

ENCLOSURE 1-NP

TO LD-83-010

STATISTICAL COMBINATION

OF

UNCERTAINTIES

PART II

Uncertainty Analysis of Limiting Safety System Settings C-E System 80 Nuclear Steam Supply Systems

REACTOR DESIGN

JANUARY 1983

Combustion Engineering, Inc.
Nuclear Power Systems
Windsor, Connecticut

LEGAL NOTICE

THIS REPORT WAS PREPARED AS AN ACCOUNT OF WORK SPONSORED BY COMBUSTION ENGINEERING, INC. NEITHER COMBUSTION ENGINEERING NOR ANY PERSON ACTING ON ITS BEHALF:

A. MAKES ANY WARRANTY OR REPRESENTATION, EXPRESS OR IMPLIED INCLUDING THE WARRANTIES OF FITNESS FOR A PARTICULAR PURPOSE OR MERCHANTABILITY, WITH RESPECT TO THE ACCURACY, COMPLETENESS OR USEFULLNESS OF THE INFORMATION CONTAINED IN THIS REPORT, OR THAT THE USE OF ANY INFORMATION, APPARATUS, METHOD, OR PROCESS DISCLOSED IN THIS REPORT MAY NOT INFRINGE PRIVATELY OWNED RIGHTS; OR

B. ASSUMES ANY LIABILITIES WITH RESPECT TO THE USE OF, OR FOR DAMAGES RESULTING FROM THE USE OF, ANY INFORMATION, APPARATUS, METHOD, OR PROCESS DISCLOSED IN THIS REPORT.

ABSTRACT

Part II of the Statistical Combination of Uncertainties (SCU) reports describes the methodology used for statistically combining uncertainties involved in the determination of the Linear Heat Rate (LHR) and Departure from Nucleate Boiling Ratio (DNBR) Limiting Safety System Settings (LSSS) for the Combustion Engineering (C-E) Nuclear Steam Supply Systems (NSSS). The overall uncertainty factors assigned to LHR and DNB Overpower Margin (DNB-OPM) establish that the adjusted LHR and DNB-OPM are conservative at a 95/95 probability/confidence level throughout the core cycle with respect to actual core conditions.

The Statistical Combination Of Uncertainties reports describe a method for statistically combining uncertainties. Part I* of this report describes the statistical combination of system parameter uncertainties in thermal margin analyses. Part II of this report describes the statistical combination of state parameter and modeling uncertainties for the determination of the LSSS overall uncertainty factors. Part III of this report describes the statistical combination of state parameter and modeling uncertainties for the determination of the Limiting Conditions for Operation (LCO) overall uncertainty factors.

* Submitted as Enclosure 1-P to letter LD-82-054 , A. E. Scherer to D. G. Eisenhut, dated May 14, 1982.

TABLE OF CONTENTS

LIST OF TABLES

LIST OF FIGURES

DEFINITION OF ABBREVIATIONS

ASI	Axial Shape Index
APHPD	Axial Pseudo Hot-Pin Power Distribution
BOC	Beginning of Cycle
BPPCC	Boundary Point Power Correlation Coefficient
CDF	Cumulative Distribution Function
C-E	Combustion Engineering
CEA	Control Element Assembly
CETOP	C-E Thermal On-Line Program
CETOP-D	Off-Line DNB-OPM Algorithm for Safety Analysis
CETOP-1	On-Line DNB-OPM Algorithm Used in Core Simulator and COLSS
CETOP-2	On-Line DNB-OPM Algorithm Used in CPC
COLSS	Core Operating Limit Supervisory System
CPC	Core Protection Calculator
DNB	Departure from Nucleate Boiling
DNBR	DNB Ratio
DNB-OPM	DNB Over Power Margin
EOC	End of Cycle
ESFAS	Emergency Safety Features Actuation System
Fq	Three Dimensional Power Peaking Factor
Fxy	Planar Radial Power Peaking Factor
LCO	Limiting Conditions for Operation
LHR	Linear Heat Rate (kw/ft)
LOCA	Loss of Coolant Accident
LSSS	Limiting Safety System Setting(s)
MOC	Middle of Cycle
NSSS	Nuclear Steam Supply System
PDF	Probability Distribution Function
PHPD	Pseudo Hot-Pin Power Distribution
PLR	Partial Length Rod
RCS	Reactor Coolant System
RPS	Reactor Protection System
RSF	Rod Shadowing Factor
RSPT	Reed Switch Position Transmitter

SAFDL	Specified Acceptable Fuel Design Limits
SCU	Statistical Combination of Uncertainties
TSF	Temperature Shadowing Factor

1.0 INTRODUCTION

1.1 PURPOSE

The purpose of this report is to describe the methodology used for statistically combining uncertainties associated with the LHR and DNBR LSSS[1]. All uncertainty components considered in the determination of the overall uncertainty factors for LHR and DNB-OPM are listed as follows:

1. Uncertainty in ex-core detector signal measurement
2. Uncertainty in Control Element Assembly(CEA) position measurement
3. Uncertainties in temperature, pressure, and flow measurements
4. Uncertainty in Core Protection Calculator (CPC)[1] LHR calculation due to the CPC power distribution synthesis for CPC LHR algorithm
5. Uncertainty in CPC DNB-OPM calculation due to the CPC power distribution synthesis for CPC DNB-OPM algorithm
6. Uncertainty in CPC DNB-OPM algorithm with respect to safety analysis DNB-OPM algorithm
7. Uncertainty in measurement of planar radial peaking factors using CECOR
8. Computer processing uncertainty
9. Startup test acceptance band uncertainties
10. Fuel and poison rod bow uncertainties
11. Global axial fuel densification uncertainty
12. Engineering factor due to manufacturing tolerance.

1.2 BACKGROUND

The plant protection system in operation on the C-E NSSS is composed of two sub-systems:

1. an Engineered Safety Features Actuation System (ESFAS), and
2. a Reactor Protection System (RPS)

The CPC initiates two of the ten trips in the reactor protection system, the low DNBR trip and the high local power density trip. The RPS assesses the LHR and DNBR LSSS as a function of monitored reactor plant parameters. The CPC uses these monitored parameters as input data and calculates the on-line LHR and DNBR margin to trip limits. A list of variables which affect the CPC calculation of LHR and DNBR in terms of the LHR and DNBR LSSS is given in Table 1-1.

These two protective functions assure safe operation of a reactor in accordance with the criteria established in 10CFR50 Appendix A (Criteria Number 10, 20, and 25)[2]. The LSSS, combined with the LCO[3], establishes the thresholds for automatic protection system actions to prevent the reactor core from exceeding the Specified Acceptable Fuel Design Limits (SAFDL) on centerline fuel melting and Departure from Nucleate Boiling (DNB). A more detailed discussion of CPC may be found in Reference 1.

A stochastic simulation of particular reactor parameters was used to evaluate uncertainties in earlier C-E analog protection systems[4] (Calvert Cliffs Unit 1 and 2)[5]. A similar method was also employed to evaluate state parameter response functions and their uncertainties in relation to the LHR and DNBR LSSS for Arkansas Unit 2, Cycle 2[6]. Results obtained from the stochastic simulation were used to obtain penalty factors for the CPC three dimensional peaking factor (Fq) and DNB-OPM calculations to ensure conservative plant operation.

1.3 REPORT SCOPE

The scope of this report encompasses the following objectives:

1. to describe the methods used for statistically combining uncertainties applicable to the LHR and DNBR LSSS;
2. to evaluate the aggregate uncertainties as they are applied in the calculation of LHR and DNBR.

The probability distribution functions associated with the uncertainties defined in Section 1.1 are analyzed to obtain the LHR and DNB-OPM overall uncertainty factors based on a 95/95 probability/confidence tolerance limit. The methods used for the determination of uncertainties on the power

measurement, the core average Axial Shape Index (ASI), and the hot-pin ASI are also described since these parameters are used in the determination of the overall uncertainty factors.

The methods presented in this report are applicable to C-E System 80 NSSS.

1.4 SUMMARY OF RESULTS

The analysis techniques described in Section 2.0 were applied to C-E System 80 NSSS. The stochastic simulation program results in overall uncertainties for the LHR LSSS and the DNBR LSSS of [%] and [%] , respectively, at a 95/95 probability/confidence level.

TABLE 1-1

VARIABLES AFFECTING THE LHR AND DNBR LSSS

LHR

1. Core Power
2. Axial Power Distribution
3. Radial Power Distribution

DNBR

1. Core Power
2. Axial Power Distribution
3. Radial Power Distribution
4. Core Coolant Inlet Temperature
5. Core Coolant Pressure
6. Primary Coolant Mass Flow

2.0 ANALYSIS

2.1 GENERAL

The following sections describe the impact of the uncertainty components on the system parameters, the state parameters, and the modeling that affect the LHR and DNBR LSSS. The effects of all individual uncertainties on the LSSS overall uncertainty factors for LHR and DNBR are also discussed. In addition, this chapter presents analyses performed to determine overall uncertainty factors which are applied to the CPC calculations of the LHR and DNB-OPM to ensure a 95/95 probability/confidence level that the calculations are conservative.

2.2 OBJECTIVES OF ANALYSIS

The objectives of the analysis reported herein are:

1. to document the stochastic simulation technique used in the overall uncertainty analysis associated with the LHR and DNBR LSSS and
2. to determine LHR and DNB-OPM overall uncertainty factors on the basis of a 95/95 probability/confidence level that the "adjusted" LHR and DNB-OPM (i.e., the CPC synthesized value corrected by the respective overall uncertainty factor) will be conservative throughout the core cycle with respect to actual core conditions.

2.3 ANALYSIS TECHNIQUES

2.3.1 GENERAL STRATEGY

The uncertainty analyses were performed by comparing the three-dimensional peaking factor (Fq) and DNB-OPM obtained from the reactor core simulator[1] to those calculated by the CPC as shown in Figures 2-1 and 2-2. The reactor core simulator generates the three-dimensional core power distributions which reflect changes in typical plant operating conditions. F_q and DNB-OPM modeling uncertainties are statistically combined with other uncertainties in calculating CPC overall uncertainty factors for LHR and DNB-OPM. The uncertainty analysis performed in this report also involves the stochastic simulation of the state parameter measurement uncertainties for the LHR and DNB-OPM calculations. The neutronic and thermal-hydraulic input parameters that

are statistically modeled[4] are given in Table 2-1. The detailed description of the individual measurement uncertainties is presented in Appendix A. The on-line to off-line thermal-hydraulic algorithm uncertainty section is also presented in Appendix A.

Approximately twelve hundred (1200) cases of power distributions at each of three burnups (BOC, MOC, EOC) were used in the determination of the overall uncertainty factors for the LHR and DNB-OPM. These cases were chosen to encompass steady state and quasi-steady state plant operating conditions throughout the cycle lifetime. Power distributions were generated by changing power levels (20-100%), CEA configurations (first two lead banks full in to full out, PLR-90% inserted to full out), and xenon and iodine concentration (equilibrium, load maneuver, oscillation).

The power measurement errors used for the LHR and DNB-OPM calculations are obtained from the CPC core power synthesis error, the secondary calorimetric power measurement error, the secondary calorimetric power to the CPC power calibration allowance, and a thermal power transient offset.* The detailed description of these uncertainty factors is given in Appendix B. The method used for the calculation of the core average ASI and hot-pin ASI uncertainties is described in Appendix C.

2.3.2 LHR LSSS STATISTICAL METHODS

The reactor core simulator was used to generate the hot-pin power distributions which served as the basis for comparison in establishing the uncertainty factors documented in this report. The CPC synthesized Fq is compared with that of the reactor core simulator Fq. Figure 2-1 illustrates the calculational sequence employed in the Fq modeling uncertainty analysis. The Fq modeling error (X_F^i) between the CPC synthesized Fq and the actual Fq is defined as:

$$X_F^i = \frac{(\text{"SYN" Fq})^i}{(\text{"ACTUAL" Fq})^i} - 1 \qquad (2\text{-}1)$$

* This error component accounts for the error in the CPC power calculation during design basis events.

where ("SYN" Fq)^i and ("ACTUAL" Fq)^i are the CPC Fq and the reactor core simulator Fq for the i-th case. The Fq errors are analyzed for each case of each time-in-life. Approximately 1200 cases are analyzed at each time-in-life (BOC, MOC, and EOC).

The mean Fq error ($\overline{X_F}$) and the standard deviation (σ_F) of the Fq error can be calculated from:

$$\overline{X}_F = \frac{\sum_{i=1}^{N} X_F^i}{N} \qquad (2\text{-}2a)$$

$$\sigma_F = \left(\frac{\sum_{i=1}^{N} (X_F^i - \overline{X}_F)^2}{N-1} \right)^{1/2} \qquad (2\text{-}2b)$$

where N = sample size

Since the mean and standard deviation are estimated from the data, the one-sided tolerance limit can be constructed from the K factor. For normal distributions, one-sided tolerance limit factor, K, is a number which accounts for the sampling variations in the mean ($\overline{X_F}$) and the standard deviation (σ_F). A normality test of the error distribution is performed by using the D-prime statistic value[7-8] to justify the assumption of a normal distribution.

The $K_{95/95}$ factor for a normal distribution[8,9] is calculated as:

$$K = \frac{K_{1-\alpha} + \sqrt{K_{1-\alpha}^2 - ab}}{a} \qquad (2\text{-}3a)$$

where

$$a = 1 - \frac{K_\alpha^2}{2(N-1)} \qquad (2\text{-}3b)$$

$$b = K_{1-p}^2 - \frac{K_\alpha^2}{N} \qquad (2\text{-}3c)$$

K_{1-p} = percentiles of a normal distribution for the probability P (1.645 for 95% probability).

K_α = percentiles of a normal distribution for the confidence coefficient (1.645 for 95% confidence).

N = sample size

If the error distribution is normal, the upper and lower one-sided 95/95 tolerance limits are calculated using the following equations:

$$\text{Lower 95/95 tolerance limit} = \overline{X} - K_{95/95}\sigma \qquad (2\text{-}4a)$$

$$\text{Upper 95/95 tolerance limit} = \overline{X} + K_{95/95}\sigma \qquad (2\text{-}4b)$$

where $\overline{X}$, σ, and $K_{95/95}$ are the sample mean, standard deviation, and one-sided tolerance limit factor, respectively.

If the error is not normally distributed, one-sided 95/95 tolerance limits are calculated by using non-parametric techniques[

] The locator L is calculated from the following equation which is derived from the methods in Reference 10.

[ ] (2-5)

[

]

The one-sided (upper or lower) 95/95 tolerance limit is obtained by selecting the error value (from the ordered error distribution) corresponding to the locator L. A non-parametric "$K\sigma$" is calculated from equation (2-4) by using the determined one-sided tolerance limit and the known mean error.

2.3.3 DNB-OPM LSSS STATISTICAL METHODS

The three-dimensional reactor core simulator provides a hot-pin power distribution for its DNB-OPM calculation and the corresponding ex-core detector signals for the CPC power distribution algorithm. In the reactor core simulator, the DNB-OPM calculation is performed with the simplified, faster running DNB algorithm CETOP-1[11]. [

] A flowchart representing the reactor core simulator DNB-OPM calculation is shown in Figure 2-2.

The Reactor Coolant System (RCS) input temperature, pressure, and flow rate are [ ]for both the reactor core simulator and CPC. [

] Operating ranges and measurement uncertainties of the state parameters are given in Table 2-2.

The SCU program also involves a stochastic simulation of the error components associated with the DNB-OPM algorithms (on-line to off-line) . [

] The effects of the error components associated with the temperature, pressure, and flow measurements and the on-line to off-line DNB-OPM algorithm are accounted for in the determination of the CPC DNB-OPM modeling error via the SCU program.

The DNB-OPM modeling error (with SCU) is defined as:

$$X^i_D = \frac{(\text{"SYN" DNB-OPM})^i}{(\text{"ACTUAL" DNB-OPM})^i} - 1 \qquad (2\text{-}6)$$

where ("SYN" DNB-OPM)^i and ("ACTUAL" DNB-OPM)^i represent the CPC DNB-OPM and the reactor core simulator DNB-OPM for the i-th case. The DNB-OPM errors are analyzed separately for each time-in-life for conservatism. Each error distribution is tested for normality and the mean DNB-OPM error ($\bar{X}_D$), standard deviation (σ_D), and one-sided upper 95/95 tolerance limit are computed.

2.4 ANALYSES PERFORMED

2.4.1 LHR LSSS UNCERTAINTY ANALYSIS

2.4.1.1 POWER DISTRIBUTION SYNTHESIS UNCERTAINTY

The reactor core simulator calculates ex-core detector signals for the CPC power distribution synthesis. An error component for each ex-core signal is [ ] and added to

the ex-core signal. An error component of each Control Element Assembly (CEA) bank measurement (reed switch position transmitters) is obtained[ ] The CEA position error component is then added to its respective CEA bank positon. The CPC synthesizes a hot-pin power distribution (PHPD) by using (as input) the adjusted ex-core detector signals and the adjusted CEA bank positions. The CPC hot-pin power distributions are obtained by using a cubic spline fitting technique in conjunction with constants such as planar radial peaking factors (Fxy), Rod Shadowing Factors (RSF), Boundary Point Power Correlation Constants (BPPCC), Shape Annealing Matrix (SAM), and Temperature Shadowing Factors (TSF).

By comparing the reactor core simulator calculated Fq with the CPC synthesized Fq for each case, the Fq modeling errors defined in equation (2-1) are obtained. By analyzing the Fq modeling errors, the CPC modeling error distributions (histogram) of Fq are obtained for each time in cycle. The mean Fq error ($\bar{X}_F$), the standard deviation (σ_F), and the lower 95/95 tolerance limit (TL_F) for the Fq modeling uncertainty are obtained by analyzing the error distribution at each time-in-life. The Fq modeling error is composed of the uncertainties associated with the CPC power synthesis algorithm, the ex-core detector signal measurement, and the CEA position measurement.

2.4.1.2 CECOR Fxy UNCERTAINTY

In the calculation of the CPC Fq modeling uncertainty, the CPC uses predicted values of F_{xy}. The Fxy used by CPC are verified by a CECOR[14] calculation of Fxy during startup testing. Therefore, the CECOR Fxy measurement uncertainty is combined with the Fq modeling uncertainty to account for the differences between the CECOR Fxy and the actual Fxy.

The CECOR Fxy error is defined as:

$$X_{FC}^{i} = \frac{G_i - P_i}{P_i} \qquad (2\text{-}7)$$

where P_i and G_i are the actual Fxy and the CECOR calculated Fxy for the i-th case, respectively.

2.4.1.3 STARTUP TEST ACCEPTANCE BAND UNCERTAINTY

The CPC power distribution algorithm[1] requires RSF, TSF, SAM, and BPPCC as input data. These constants are assumed to be known exactly for the CPC calculation of the core hot-pin power distributions. These CPC power distribution algorithm constants are therefore verified during startup testing. The CPC constants for RSF, TSF, SAM, and BPPCC should agree with the respective measured values within the startup test acceptance criteria. The acceptance band criteria on these constants also have associated uncertainties which affect the CPC calculated Fq and DNB-OPM. Penalty factors due to RSF, TSF, SAM, and BPPCC uncertainties are considered in the CPC overall uncertainty analysis.

In order to obtain the penalty factor due to RSF uncertainty, the CPC and reactor core simulator Fq calculations for base case are performed using the nominal CPC data base constants for twelve hundred (1,200) cases at each time-in-life. The RSF value (R) for a given rod configuration is changed from the CPC data base constant value (base case value) and the CPC Fq are then calculated with this changed RSF value ($R + \Delta R$). [

]

[

(2-8a)

(2-8b)

]

The penalty factors due to the TSF, SAM, and BPPCC uncertainties are also obtained by following a similar procedure.

The startup test acceptance band uncertainty (PS) is calculated by statistically combining the penalty factors due to RSF, TSF, SAM, and BPPCC uncertainties and is represented by the following equation:

[ ] (2-9)

where

[ ]

2.4.1.4 OTHER UNCERTAINTY FACTORS

Axial Fuel Densification Uncertainty

The axial fuel densification uncertainty factor[15] considers the global effect of the shrinkage of the fuel pellet stack, due to heating and irradiation, on the CPC Fq calculations. [ ]

Fuel and Poison Rod Bow Uncertainties

The fuel and poison rod bow uncertainties[16] consider the effect of "bowing" of the fuel and poison rods,due to heating and irradiation,on the CPC Fq calculations. These factors will be part of the composite Fq modeling uncertainty.

Computer Processing Uncertainty

The computer processing uncertainty considers the effect of the computer machine precision of the C-E 7600 computer and the on-site computer on the CPC Fq calculations. The computer processing uncertainty will be part of the composite Fq modeling uncertainty.

Engineering Factor Uncertainty

The engineering factor considers the effect on the CPC Fq calculation due to fuel manufacturing tolerance[15]. This factor will be part of the composite F_q modeling uncertainty.

2.4.1.5 OVERALL LHR LSSS UNCERTAINTY FACTOR

An overall CPC Fq uncertainty factor is determined by combining all lower 95/95 probability/confidence tolerance limits of the error components. This overall uncertainty factor includes the composite Fq modeling uncertainty, the startup test acceptance criteria uncertainty, and the axial fuel densification uncertainty. Figure 2-3 shows the calculational sequence to determine an overall LHR LSSS uncertainty factor.

The Fq modeling error (X_{FM}^i) defined in equation (2-1) can be rewritten as:

$$X_{FM}^i = \frac{C_i - F_i}{F_i} \qquad (2\text{-}10)$$

where F_i and C_i are the reactor core simulator calculated Fq and the CPC inferred value of Fq for the i-th case, respectively. A composite error ($X_{FT}{}^i$) of the Fq modeling uncertainty and the CECOR Fxy measurement uncertainty can be deterministically calculated as follows:

$$X_{FT}^i = \left(\frac{C_i}{F_i}\right)\left(\frac{G_i}{P_i}\right) - 1 \qquad (2\text{-}11)$$

By applying equations (2-7) and (2-10), this leads to:

$$X_{FT}{}^i = X_{FM}{}^i + X_{FC}{}^i + (X_{FM}{}^i * X_{FC}{}^i) \qquad (2\text{-}12)$$

The mean of the composite Fq modeling uncertainty is determined by:

$$\bar{X}_{FT} = \bar{X}_{FM} + \bar{X}_{FC} + (\bar{X}_{FM} * \bar{X}_{FC}) \qquad (2\text{-}13)$$

The "Kσ" of the composite Fq modeling uncertainty is determined by combining the "Kσ" for CECOR Fxy ($K\sigma_{FC}$), CPC power distribution synthesis ($K\sigma_{FM}$), engineering factor ($K\sigma_{FE}$), rod bow penalties ($K\sigma_{pF}$, $K\sigma_{pp}$), computer processing ($K\sigma_{CP}$), and FLARE/ROCS[1] modeling error ($K\sigma_{FR}$)*:

[ ] (2-14)

The resultant composite Fq modeling penalty factor (PM_F) is determined by using the lower 95/95 composite tolerance limit (TL_F) for Fq as follows:

$$PM_F = \frac{1}{1 + TL_F} \qquad (2\text{-}15)$$

where

$$TL_F = \bar{X}_{FT} - (K\sigma)_{FT} \qquad (2\text{-}16)$$

The lower tolerance limit is used to assure conservative CPC F_q calculations at a 95/95 probability and confidence level.

The last step to determine an overall Fq uncertainty factor (BERR3) is to combine the composite modeling uncertainty (PM_F), the startup acceptance criteria uncertainty (PS) and the axial fuel densification uncertainty (PA).

Consequently,

[ ] (2-17)

*See Appendix A.4 .

The LSSS LHR overall uncertainty factor (BERR3) is used [ ] on the CPC calculated LHR (KW/FT):

$$\text{CPC "SYN" LHR} * (\text{BERR3})_{95/95} > \text{"ACTUAL" LHR} \qquad (2\text{-}18)$$

Use of the overall uncertainty factor (BERR3) for the CPC calculated LHR assures at least a 95% probability, at a 95% confidence level, that the CPC LHR will be larger than the "ACTUAL" LHR.

2.4.2 DNB-OPM LSSS UNCERTAINTY ANALYSIS

2.4.2.1 DNB-OPM MODELING UNCERTAINTY WITH SCU

The CPC DNB-OPM modeling uncertainty with SCU is made up of uncertainties associated with power distribution synthesis, DNB algorithm, ex-core detector signal measurement, CEA position measurement, RCS temperature measurement, RCS pressure measurement, and RCS flow measurement. In order to include the RCS inlet temperature, pressure, and flow rate effects in the DNB-OPM modeling uncertainty, a [ ] program is employed. [

]

By comparing the reactor core simulator calculated DNB-OPM with the CPC calculated DNB-OPM for each case, the DNB-OPM modeling error is obtained. The mean of the DNB-OPM modeling error is represented by:

[ ] (2-19)

[

] The detailed description of the SCU DNB-OPM modeling uncertainty is presented in Appendix A.3.

2.4.2.2 DYNAMIC PRESSURE UNCERTAINTY

Core inlet temperature, primary system pressure, and primary coolant flow rate affect the calculation of DNB-OPM. Errors associated with the static temperature, pressure, and flow measurements must be accounted for in the calculation of the net CPC DNB-OPM uncertainty. However, these errors are implicitly included in the modeling uncertainty via the SCU program .

For the CPC DNB-OPM calculation during a transient, the pressurizer pressure sensed by the precision pressure transducer is adjusted to get RCS pressure by considering dynamic pressure compensation offset. In order to take account for RCS pressure change during a transient, an additional uncertainty in the DNB-OPM overall uncertainty analysis is considered.

The uncertainty for the dynamic pressure may be represented by:

[ ] (2-20)

where

[ ]

By using the CETOP-D code, the calculation of DNB-OPM is carried out over the parameter range of plant operation presented in Table 2-2. The wide ranges of radial peak and ASI are also considered in this analysis. [

]

[ ] (2-21)

[ ]

The dynamic pressure compensation offset (ΔP_D) is defined as the pressure difference between sensor measured pressure and the RCS pressure during a transient. In order to calculate ΔP_D, the RCS pressure change rate during the worst transient (such as a pressurizer spray valve malfunction) is calculated. Then, the dynamic pressure compensation is obtained by multiplying the pressure change rate by the total sensor delay time.

[ ]

2.4.2.3 OTHER UNCERTAINTY FACTORS

DNBR Computer Processing Uncertainty

The computer processing uncertainty considers the effect of the off-line (CDC 7600 computer) to the on-line computer machine precision on the CPC DNB-OPM calculations. The computer processing uncertainty is represented by the term $(K\sigma)_{DT}$ and is part of the DNB-OPM composite modeling uncertainty. This computer processing uncertainty ($K\sigma_{CP}$) is calculated by using the following equation:

[ ] (2-22)

[ ]

[ ] (2-23)

Startup Test Acceptance Band Uncertainty

The startup test acceptance band uncertainty for DNB-OPM is determined by the same method described in Section 2.4.1.3.

Fuel and Poison Rod Bow Uncertainties

The fuel and poison rod bow uncertainties for DNB-OPM are determined by the same method described in Section 2.4.1.4.

System Parameter Uncertainties

In order to determine the minimum DNBR (MDNBR) limit, C-E thermal margin methods utilize the detailed TORC code with the CE-1 DNB correlation[12]. The MDNBR for LSSS includes the uncertainties associated with system parameters which describe the physical system. These system parameters are composed of reactor core geometry, pin-by-pin radial power distributions, inlet and exit flow boundary conditions, etc. In the statistical combination of system parameter uncertainties[17], the following uncertainties are combined statistically in the MDNBR limit:

1. Inlet flow distribution uncertainties
2. Fuel pellet density uncertainties
3. Fuel pellet enrichment uncertainties
4. Fuel pellet diameter uncertainties
5. Random and systematic uncertainties in fuel clad diameter
6. Random and systematic uncertainties in fuel rod pitch
7. DNB correlation uncertainties

The SCU MDNBR limit provides, at a 95/95 probability and confidence level, that the limiting fuel pin will avoid DNB. Since the SCU MDNBR limit includes system parameter uncertainties as described in Part I of this report, these uncertainties are not considered in the determination of the CPC DNB OPM overall uncertainty factor.

2.4.2.4 OVERALL DNB-OPM LSSS UNCERTAINTY FACTOR

The overall CPC uncertainty factor for DNB-OPM (BERR1) is determined by combining all one-sided (upper) 95/95 probability/confidence tolerance limits. This overall uncertainty factor is made up of the composite DNB-OPM modeling

uncertainty, the dynamic pressure uncertainty, and the startup test acceptance band uncertainty. Figure 2-3 illustrates the calculational sequence to determine the overall DNB-OPM LSSS uncertainty factor.

A composite DNB-OPM modeling was obtained by following a similar strategy to that used for the Fq uncertainty analysis. The CECOR Fxy measurement uncertainty was calculated in terms of DNB-OPM units using the sensitivity of DNB-OPM to Fxy $\{ \partial(\%DNB\text{-}OPM)/\partial(\%Fxy) \}$. The mean of the CECOR Fxy error is given by:

[ ] (2-24a)

and the CECOR F_{xy} "$K\sigma$" is given by:

[ ] (2-24b)

The composite mean error for the composite DNB-OPM modeling uncertainty can then be calculated as:

$$\overline{X}_{DT} = \overline{X}_{DM} + \overline{X}_{DC} + \overline{X}_{DM} * \overline{X}_{DC} \qquad (2\text{-}25)$$

The composite $(K\sigma)_{DT}$ is made up of uncertainties for DNB-OPM modeling algorithm ($K\sigma_{DM}$), CECOR Fxy ($K\sigma_{DC}$), rod bow penalties ($K\sigma_{pF}$, $K\sigma_{pp}$), and DNBR computer processing ($K\sigma_{CP}$), and FLARE/ROCS modeling error ($K\sigma_{FR}$). Using the root-sum-square technique, this composite $(K\sigma)_{DT}$ is calculated as:

[ ] (2-26)

The upper 95/95 composite modeling tolerance limit for DNB-OPM (TL_D) is used for conservative CPC DNB-OPM calculations and determined by:

$$TL_D = \overline{X}_{DT} + (K\sigma)_{DT} \qquad (2\text{-}27)$$

The composite DNB-OPM modeling penalty factor (PM_D) can then be determined as:

$$PM_D = 1 + TL_D \qquad (2\text{-}28)$$

In order to determine an overall DNB-OPM uncertainty, the composite DNB-OPM modeling penalty factor (PM_D) is [ ] combined with the dynamic pressure penalty (PP_D) and the startup acceptance band uncertainty.

An overall DNB-OPM uncertainty factor for CPC (BERR1) is determined by combining PM_D, PP_D, and PS:

[ ] (2-29)

This LSSS DNB-OPM overall uncertainty factor (BERR1) is used [as a multiplier] on the CPC hot pin heat flux distribution used in the DNBR calculation:

$$\text{CPC "SYN" DNB-OPM} * (\text{BERR1})_{95/95} < \text{"ACTUAL" DNB-OPM} \qquad (2\text{-}30)$$

Use of the overall uncertainty factor (BERR1) for the CPC calculated DNB-OPM assures at least a 95% probability, at 95% confidence level, that the "ACTUAL" DNB-OPM will be larger than the CPC DNB-OPM.

TABLE 2-1

STATISTICALLY MODELED VARIABLES

NEUTRONICS

CEA Positions
Ex-Core Detector Signals

THERMAL HYDRAULICS

RCS Pressure
Core Inlet Temperature
Core Flow

TABLE 2-2

RANGES AND MEASUREMENT UNCERTAINTIES
OF STATE PARAMETERS

PARAMETERS	UNIT	RANGES	MEASUREMENT UNCERTAINTY
Core Inlet Coolant Temperature	(°F)	[ ]	[ ]
Primary Coolant Pressure	(PSIA)		
Primary Coolant Flow Rate	(GPM)		

Figure 2-1

CPC SIMULATION FOR F_q

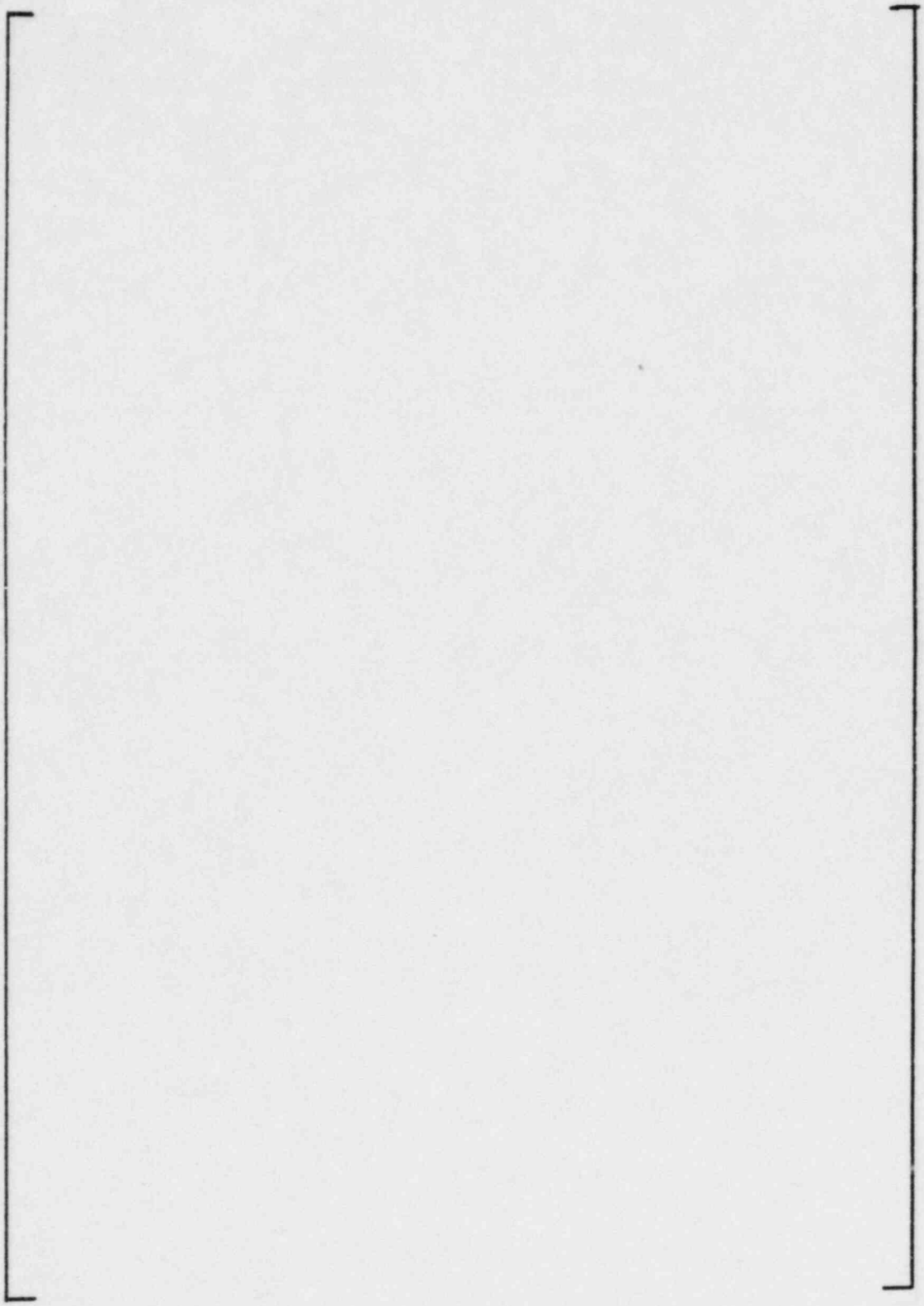

Figure 2-2

CPC SIMULATION FOR DNB-OPM

FIGURE 2-3

FLOWCHART FOR CPC OVERALL UNCERTAINTIES
FOR LHR AND DNB-OPM

3.0 RESULTS AND CONCLUSIONS

The analysis techniques described in Section 2 have been used to obtain uncertainties associated with the LHR and DNBR LSSS at a 95/95 probability/confidence level. The results of the analyses performed for C-E System 80 NSSS are presented in this section.

3.1 LHR LSSS

Following the analysis techniques described in Section 2.4.1, CPC synthesized Fq modeling errors are tabulated in Table 3-1 for the three times in core life (BOC, MOC, EOC). All time-in-life dependent Fq modeling uncertinties were considered in evaluating the overall Fq penalty. However, the time-in-life that led to the worst modeling uncertainty was used to determine the overall Fq uncertainty factor. The individual uncertainty components of the Fq overall uncertainty factor are listed in Table 3-2. Combining the uncertainties associated with the LHR LSSS results in an aggregate uncertainty of [%] at a 95/95 probability/confidence level. This overall uncertainty factor of [%], when applied to the CPC synthesized Fq, will assure that the CPC Fq will be larger than the actual Fq at a 95/95 probability/confidence level at all times during the fuel cycle.

3.2 DNBR LSSS

Following the analysis techniques presented in Section 2.4.2, the mean values, standard deviations, and upper tolerance limit of the CPC synthesized DNB-OPM modeling error were calculated and are summarized in Table 3-3. The modeling error was analyzed as a function of the time-in-life, but only the time-in-life that led to the most conservative modeling uncertainty was considered in the calculation of the overall CPC DNB-OPM uncertainty. The individual uncertainty components of the overall DNB-OPM uncertainty factor are presented in Table 3-2. Combining the uncertainties associated with the DNB-OPM LSSS gives an overall uncertainty factor of [%] at a 95/95 probability/confidence level. This overall uncertainty factor, when applied to the CPC synthesized DNB-OPM, will assure that the CPC DNB-OPM will be smaller than the actual DNB-OPM at a 95/95 probability/confidence level at all times during the fuel cycle.

TABLE 3-1

CPC SYNTHESIZED F_q MODELING ERROR[1] ANALYSIS

TIME IN CORE LIFE	NUMBER OF DATA POINTS (N)	MEAN ERROR ($\bar{X}_E$), %	STANDARD[3] DEVIATION (σ), %	95/95 TOLERANCE[2],[3] LIMIT $(TL)_F$
BOC	[			]
MOC				
EOC				

(1) $$\text{ERROR} = \left(\frac{\text{"SYN" } F_q}{\text{"ACTUAL" } F_q} - 1 \right) * 100$$

(2) See References 9 and 10. Normal or non-parametric values presented.

(3) If error distribution is determined to be non-parametric, the value for $(K\sigma)_F$ is calculated as

$$(K\sigma)_F = -(TL)_F + \bar{X}_F$$

TABLE 3-2

CONTRIBUTION OF INDIVIDUAL UNCERTAINTY
TO LSSS OVERALL UNCERTAINTY FACTORS

UNCERTAINTY		LHR LSSS	DNB-OPM LSSS
3-D Peak (Fq) Modeling(1)	$\bar{X}$	[	]
	$K\sigma$		
CECOR Fxy	$\bar{X}$		
	$K\sigma$		
Engineering Factor			
Fuel Rod Bow			
Poison Rod Bow			
Axial Densification			
Rod Shadowing			
Temperature Shadowing			
Boundary Point Power			
Shape Annealing Matrix			
Computer Processing			
DNB-OPM Modeling with SCU(2)	$\bar{X}$		
	$K\sigma$		
Dynamic Pressure			
FLARE/ROCS Modeling			

(1) includes power distribution synthesis uncertainty, ex-core signal noise, CEA position error.

(2) includes [ ] in addition to errors of (1).

TABLE 3-3

CPC SYNTHESIZED DNB-OPM MODELING ERROR[1] ANALYSIS

TIME IN CORE LIFE	NUMBER OF DATA POINTS (N)	MEAN ERROR ($\bar{X}_D$), %	STANDARD[3] DEVIATION (σ), %	95/95 TOLERANCE[2],[3] LIMIT $(TL)_D$
BOC	[			]
MOC				
EOC				

(1) $\text{ERROR} = \left(\frac{\text{"SYN" DNB-OPM}}{\text{"ACTUAL" DNB-OPM}} - 1 \right) * 100$

(2) See References 9 and 10. Normal and non-parametric values presented.

(3) If error distribution is considered non-parametric, the value for $(K\sigma)_D$ is calculated as:

$$(K\sigma)_D = (TL)_D - \bar{X}_D$$

REFERENCES

1. Combustion Engineering, Inc., "Assessment of the Accuracy of PWR Safety System Actuation as Performed by the Core Protection Calculators", CENPD-170-P and Supplement, July, 1975.
2. Combustion Engineering, Inc., "System 80, Combustion Engineering Standard Safety Analysis Report (CESSAR), Final Safety Analysis Report (FSAR)", March 31, 1982.
3. Combustion Engineering, Inc., "COLSS, Assessment of the Accuracy of PWR Operating Limits as Determined by the Core Operating Limit Supervisory System", CENPD-169-P, July, 1975.
4. Combustion Engineering, Inc., "Statistical Combination of Uncertainties Methodology", Part-I and III, CEN-124(B)-P, 1980.
5. Docket No. 50-317, "Safety Evaluation by the Office of Nuclear Regulation for Calvert Cliffs Unit 1, Cycle 3", June 30, 1978.
6. Combustion Engineering, Inc., "Response to Questions on Documents Supporting The ANO-2 Cycle 2 Licensing Submittal", CEN-157(A)-P, Amendment 1, June, 1981.
7. American National Standard Assessment of the Assumption of Normality, ASI-N15-15, October, 1973.
8. Sandia Corporation, "Factors for One-Sided Tolerance Limits and for Variable Sampling Plans", SCR-607, March, 1963.
9. C. L. Crow, et al, "Statistical Manual", Dover Publications, Inc., New York, 1978.
10. R. E. Walpole and R. H. Myers, "Probability and Statistics for Engineers and Scientists 2ed", Maconillan Publishing Company, Inc., New York, 1978.
11. Chong Chiu, "Three-Dimensional Transport Coefficient Model and Prediction-Correction Numerical Method for Thermal Margin Analysis of PWR Cores", Nuclear Eng. and Design, P103-115, 64 , March, 1981.
12. Combustion Engineering, Inc., "CETOP-D Code Structure and Modeling Methods for San Onofre Nuclear Generating Station Units 2 and 3", CEN-160(S)-P, May, 1981.
13. Combustion Engineering, Inc., "Functional Design Specification for a Core Protection Calculator", CEN-147(S)-P, January, 1981.
14. Combustion Engineering, Inc., "INCA/CECOR Power Peaking Uncertainty", CENPD-153-P, Rev. 1-P-A, May, 1980.

15. Combustion Engineering, Inc., "Fuel Evaluation Model", CENPD-139-P, October, 1974.
16. Combustion Engineering, Inc., "Fuel and Poison Rod Bowing", CENPD-225-P and Supplements, June, 1978.
17. Combustion Engineering, Inc., "Statistical Combination of Uncertainties, Combination of System Parameter Uncertainties in Thermal Margin Analyses for System-80", Enclosure 1-P to LD-82-054, May 1982.

APPENDIX A

A.1 Detector Signal Measurement and CEA Bank Position Measurement Uncertainties

In the SCU program, error components of ex-core detector signals are [ ] This error component is then added to the ex-core signal generated by the reactor core simulator and is used as input to the CPC power distribution algorithm.

The location of each CEA bank is measured using the Reed Switch Position Transmitters (RSPT). An error component of each CEA bank measurement is selected [ ] The sampled error is then added to the respective CEA bank position for input to the CPC power distribution algorithm.

A.2 State Parameter Measurement Uncertainties

The on-line DNB-OPM algorithm[A-1] used for CPC requires primary system pressure, core inlet temperature, core power, primary coolant flow rate, and hot pin power distribution as input. Since pressure, temperature, and flow affect the calculation of DNB-OPM, errors associated with these state parameters must be accounted for in the CPC DNB-OPM uncertainty analysis. [

] This procedure allows for direct simulation of the effects of the CPC on-line inlet temperature, pressure, and flow measurement and their respective uncertainties on the calculation of the CPC DNB-OPM. Therefore, DNB-OPM uncertainties with respect to temperature, pressure, and flow are implicitly accounted for in the DNB-OPM modeling uncertainty.

A.3 DNB-OPM Algorithm Uncertainties

Ideally the DNB-OPM overall uncertainty calculation would use three distinct thermal hydraulic algorithms. The off-line safety-analysis algorithm (CETOP-0) represents the base-line DNB-OPM calculation. CETOP-1[A-2] and CETOP-2[A-1] are simplified versions of CETOP-0 and perform the on-line thermal hydraulic calculations for the plant monitoring and protection systems, respectively. [

] The actual calculational scheme is shown in Figure A-1.

[

]

A.4 FLARE/ROCS Modeling Error

The reactor core simulator uses the FLARE neutronic model to predict representative power distributions. The FLARE model is tuned to a more accurate and rigorous ROCS code. The FLARE/ROCS modeling error takes account for the effect of the FLARE modeling uncertainty on the reference LHR and DNB-OPM calculations.

A.5 References for Appendix A

A-1 Combustion Engineering, Inc., "Functional Design Specification for a Core Protection Calculator", CEN-147(S)-P , February, 1981.

A-2 Chong Chiu, "Three-Dimensional Transport Coefficient Model and Prediction-Correction Numerical Method for Thermal Margin Analysis of PWR Cores", Nuclear Eng. and Design, P103-115, 64 , March, 1981.

A-3 M. G. Kendall and A. Stuart, "The Advanced Theory of Statistics, Vol. II", Hafner Publishing Company, New York, 1961, p. 457.

Figure A-1

DNB-OPM ALGORITHMS

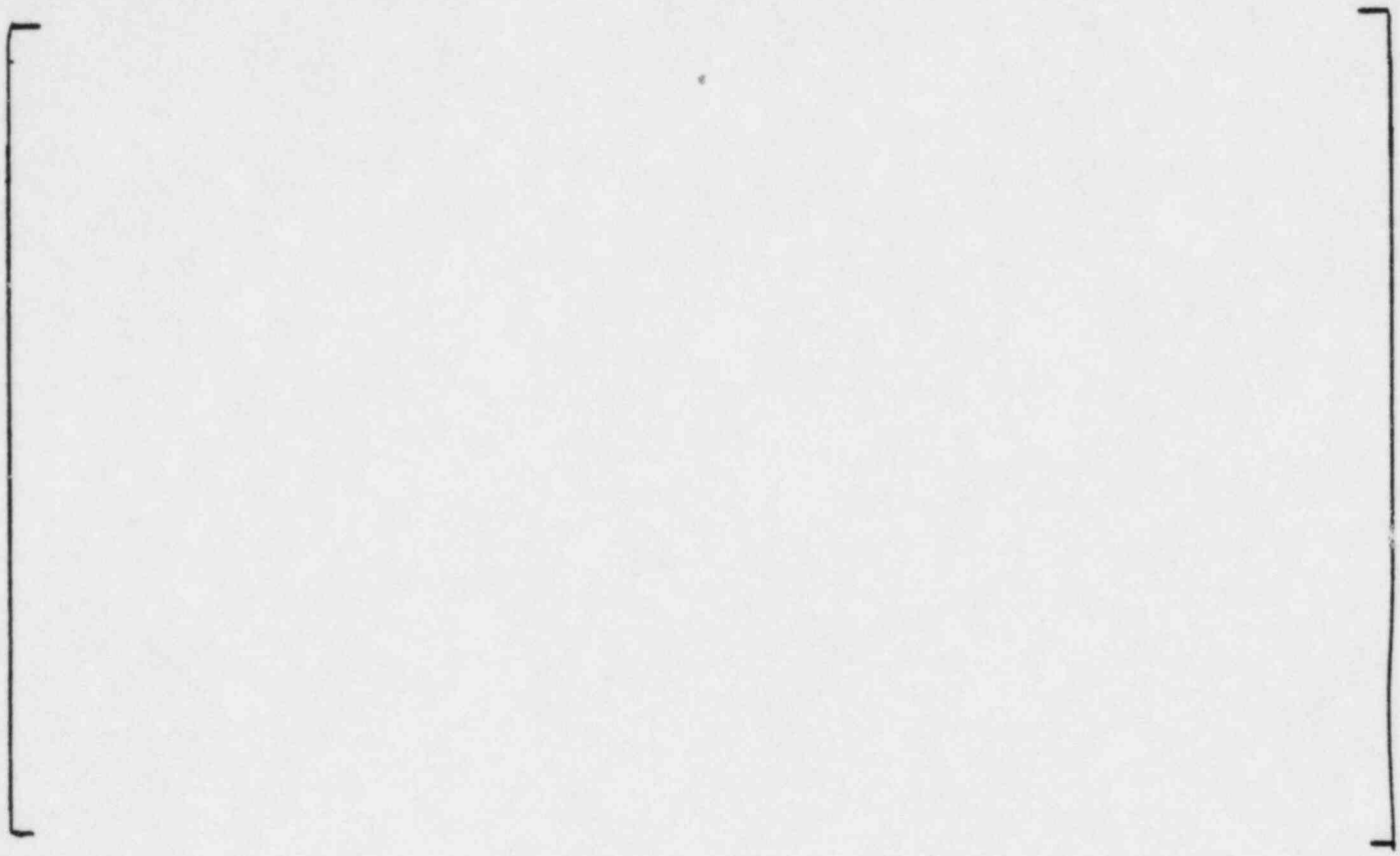

APPENDIX B

Core Power Level Measurement Uncertainty

The CPC utilizes two different calculations of core power, thermal power and neutron flux power, for the LHR and DNB-OPM calculation. The CPC thermal power is calculated based on the reactor coolant temperature and the reactor coolant mass flow rate. The CPC neutron flux power is calculated based on the sum of the tri-level ex-core detector signals. The core power level measurement uncertainty factors are obtained from the CPC neutron flux synthesis error, the secondary calorimetric power measurement error, the secondary calorimetric power to the CPC power calibration allowance, and the thermal power transient offset.

The CPC thermal power measurement error is determined by deterministically combining the secondary calorimetric power measurement error, the secondary calorimetric power to the CPC power calibration allowance, and the thermal power transient offset. The secondary calorimetric power measurement error (X_{sc}) is obtained as follows:

[

]

The secondary calorimetric power to the CPC power calibration allowance and the thermal power transient offset used for C-E system 80 NSSS are [%] and [%], respectively. The thermal power measurement uncertainty factor for the CPC DNB-OPM calculation (BERRO) is determined by selecting the maximum value of the thermal power measurement errors for the core power range (0-130% full power). [

]

The CPC neutron flux power measurement error is calculated by deterministically combining the neutron flux power synthesis error, the secondary calorimetric power measurement error, and the secondary calorimetric power to the CPC power calibration allowance. The one-sided (lower) tolerance limit for the CPC neutron flux power synthesis error (at a 95/95 probability/confidence level) is obtained by analyzing each neutron flux power distribution for each time-in-life. The CPC neutron flux power synthesis error for C-E System 80 NSSS is presented in Table B-1. The neutron flux power measurement uncertainty factor for the CPC DNB-OPM calculation (BERR2) is determined by selecting the maximum value of the neutron flux power measurement error for the core power range (0-130% full power). [

]

[

]

The core power measurement uncertainty factor for the LHR calculation (BERR4) is obtained by selecting the largest of the CPC thermal power errors or the CPC neutron flux power errors over the core power range from 0-130% full power. [

]

The CPC power measurement errors for C-E System 80 are given in Table B-2 as a function of power.

TABLE B-1

CPC POWER SYNTHESIS ERROR* ANALYSIS

BURNUP	NUMBER OF DATA POINTS	MEAN ERROR (%)	STANDARD DEVIATION (%)	LOWER 95/95 TOLERANCE LIMIT
BOC	[			]
MOC				
EOC				

* Power Synthesis Error $= \left(\frac{\text{CPC POWER - STIMULATOR POWER}}{\text{STIMULATOR POWER}} \right)$

TABLE B-2

POWER MEASUREMENT UNCERTAINTY AS A FUNCTION OF POWER

TRUE POWER (%)	CALORIMETRIC ERROR (%)	FOR DNB-OPM		FOR LHR
		THERMAL POWER ERROR (%)	NEUTRON FLUX POWER ERROR (%)	POWER ERROR** (%)
0	[			]
10				
20				
30				
40				
50				
60				
70				
80				
90				
100				
110				
120				
130				

*Largest value.

**Power error for LHR uses a transient power offset of [ ].

APPENDIX C

Axial Shape Index Uncertainty

The axial shape index (ASI) for the core average and the hot-pin power distributions is computed from the power generated in the lower and upper halves of the core:

$$ASI = \frac{P_L - P_U}{P_L + P_U} \qquad (C\text{-}1)$$

where

P_L and P_U are, respectively, power in the lower half and the upper half of the core.

The ASI error is defined by:

$$\text{ASI Error} = \text{CPC ASI} - \text{Reactor Core Simulator ASI} \qquad (C\text{-}2)$$

The core average and hot-pin ASI uncertainty analyses are performed by comparing the CPC synthesized ASI and the reactor core simulator ASI. The resulting error distributions are analyzed to obtain the upper and lower 95/95 tolerance limits. The hot-pin ASI and the core average ASI uncertainties for C-E System 80 NSSS are presented in Tables C-1 and C-2.

TABLE C-1

HOT-PIN ASI ERROR* ANALYSIS

BURNUP	NUMBER OF DATA POINTS	MEAN ERROR (%)	STANDARD DEVIATION (%)	LOWER 95/95 LIMIT	UPPER 95/95 LIMIT
BOC	[				]
MOC					
EOC					

* ASI ERROR = (CPC ASI - SIMULATOR ASI)

TABLE C-2

CORE AVERAGE ASI ERROR* ANALYSIS

BURNUP	NUMBER DATA POINTS	MEAN ERROR (%)	STANDARD DEVIATION (%)	LOWER 95/95 LIMIT	UPPER 95/95 LIMIT
BOC	[				]
MOC					
EOC					

* ASI ERROR = (CPC ASI - SIMULATOR ASI)